PHYSICAL REVIEW B **67**, 155328 (2003)

Thermopower of a double quantum well based on GaAs

T. Smith,[1] M. Tsaousidou,[2] R. Fletcher,[1] P. T. Coleridge,[3] Z. R. Wasilewski,[3] Y. Feng[3]
[1]*Physics Department, Queen's University, Kingston, Ontario, Canada K7L 3N6*
[2]*Materials Science Department, University of Patras, Patras 26 504, Greece*
[3]*Microstructural Sciences, National Research Council, Ottawa, Canada K1AOR6*
(Received 12 November 2002; revised manuscript received 21 February 2003; published 30 April 2003)

The resistivity and thermopower of a double quantum well have been investigated in the temperature range 0.3−4.2 K as a function of voltage applied to a top gate. As in previous studies, the resistivity showed a strong resonance when the carrier densities in each well were approximately the same. In contrast, neither diffusion nor phonon-drag thermopower showed any sensitivity to the resonance. We have calculated the thermopower based on a model of two independent two-dimensional electron gases (2DEG's) connected in parallel. In the case of phonon-drag thermopower, S^g, it was necessary to take into account the mutual screening of the electron-phonon interaction by electrons in each layer and also the local-field correction to the static dielectric function. We find that S^g exhibits a T^5 dependence at low temperatures instead of the standard T^4 expected for single GaAs quantum wells. We also find that, for the lowest densities examined, the local-field correction enhances the magnitude of the calculated S^g by over a factor of 2, in good agreement with experiment. As a check on the model of two independent 2DEG's we have also calculated S^g at resonance taking into account interwell coupling. The calculated values of S^g so obtained are in good agreement with those obtained for uncoupled wells. This confirms the experimental result that S^g is insensitive to the resonance condition.

DOI: 10.1103/PhysRevB.67.155328 PACS number(s): 73.50.Lw, 73.40.Kp

I. INTRODUCTION

Over the last decade, double quantum wells (DQW's) coupled by tunneling have been found to exhibit a wide variety of interesting properties. If we confine ourselves to the research on transport measurements in the plane of the wells, previous work has almost invariably focused on the electrical conductivity of the wells, studied either in parallel (i.e., the wells are connected together at the contact points) or separately. The parallel conductivity shows a resonance when the two wells are adjusted to be symmetric so that their energy levels coincide (usually by one or more gates which vary the local potential seen by the wells). When the energy levels in the two wells are very different, tunneling is weak and each well contributes to the current essentially independently. At resonance the wave functions of the wells combine to form symmetric and antisymmetric states which are separated by an energy gap and the electrons spend equal times in the two wells. This averages the scattering of the electrons in the two wells and leads to an increase in the measured parallel resistance.[1,2]

Practically all the published transport work on these systems has involved only electrical resistivity. The only exceptions of which we are aware are the experimental work of Hyndman *et al.*[3] who measured the thermopower of a *p*-type DQW in strong perpendicular fields, and the calculation of Lyo[4] for the diffusion thermopower of a symmetric DQW in a parallel magnetic field.

The system studied by Hyndman *et al.*[3] had strong Coulomb interactions and the authors were primarily interested in the effect that this had on the quantum and fractional-quantum Hall effects. They also presented some data at zero field which showed that the thermopower was dominated by phonon drag.

The present work reports an investigation, both experimental and theoretical, of the thermoelectric properties in zero magnetic field of an *n*-type AlGaAs/GaAs/AlGaAs DQW as the occupation of the wells is varied using a top gate. Perhaps the most interesting result is that the thermopower is found to be insensitive to the resonance condition.

In most of our theoretical work we have modeled the system as two independent two-dimensional electron gases (2DEG's) connected in parallel. We give an elementary account of the diffusion thermopower, but most of our calculations have focused on the phonon-drag contribution, S^g. In contrast to resistivity and diffusion thermopower, which are largely controlled by elastic impurity scattering, S^g is known to be determined by the momentum relaxation time due to electron-phonon (e-p) scattering.[5,6] The e-p coupling in each layer is screened by the electrons in the opposite layer. This significantly reduces the magnitude of S^g at low T and also leads to $S^g \propto T^5$ at the lowest temperatures examined ($T < 0.4$ K) rather than the standard $S^g \propto T^4$ appropriate to single wells.[7–9] In order to check the validity of the model of two independent 2DEG's we have also carried out a detailed calculation of S^g at resonance, taking into account the effects of interwell coupling on the electronic wave functions. We find that the calculated values of S^g in both theoretical treatments are in good agreement.

A considerable amount of theoretical work[10–15] has focused on the dielectric properties of dilute gases when the random-phase approximation is no longer accurate due to exchange and correlation effects. The present work provides clear evidence for the importance of the role of the local-field correction to the static dielectric function in 2DEG's at low densities. We were able to obtain good agreement between experiment and theory only by including this correction in the calculations.

The paper is set out as follows. After discussing the experimental methods in the next section, we outline our theo-

 ©2003 The American Physical Society

retical calculations in Sec. III. This provides a framework to understand our experimental results in Sec. IV and the discussion in Sec. V. In the Appendix we present a full calculation of the phonon-drag thermopower of two coupled quantum wells at resonance. A preliminary report on this work is available in conference form.[16]

II. EXPERIMENTAL TECHNIQUES

The sample had two 18-nm GaAs wide wells separated by 3.4 nm of $Al_{0.33}Ga_{0.67}As$. A δ-doped Si layer on each side of the wells, separated by 120 nm of $Al_{0.33}Ga_{0.67}As$, provided the electrons. A top gate, consisting of a gold film on 30 nm of SiO_2, allowed the total carrier density, n_{tot}, to be increased or decreased. The sample was produced from the same wafer used by Charlebois *et al.*[17] though their experiments used a much thicker oxide for the gate. The potential and current contacts shorted the two wells so that the measured properties corresponded to the wells connected in parallel.

Measurements were made over the temperature range 0.3–4.2 K. The measured coefficients were very reproducible functions of the gate voltage if the sample was kept at liquid-nitrogen temperatures between cooldowns. All measurements were made by dc techniques. We used an EM model N11 nanovoltmeter as the voltage detector for thermopower measurements and a Keithley model 182 voltmeter for resistance measurements. Temperatures were determined by two ruthenium-dioxide, surface-mount sensors mounted on the sample by epoxy. The thermometry was checked by measuring the thermal conductivity, λ, of the sample substrate. At low temperatures ($T<0.6$ K) λ was proportional to T^3 as expected, with a phonon mean free path estimated to be about 3 mm. We expect absolute errors in the thermopower S and λ to be about 15% because of uncertainty in the spacing of the thermometers, but we mainly dealt with the quantity S/λ ($S/\lambda=-E_x/U_x$ where E_x is the electric field in the x direction and U_x the heat current density) which is independent of this spacing so the errors are smaller. The scatter on the data mainly arose from the precision with which the voltage differences across the sample could be measured. This is a few nV for thermoelectric quantities.

The calculation of the thermopower required the densities and the mobilities of the carriers in each well. We have experimentally determined these in some detail[18] as a function of gate voltage. For the present purposes it is a sufficiently good approximation to assume that the density of carriers in the upper well, n_u, was a linear function of gate voltage, V_g, given approximately by $n_u=(2.06V_g+0.94)\times10^{15}\ \mathrm{m}^{-2}$ and that of the lower well, $n_l=0.86\times10^{15}\ \mathrm{m}^{-2}$, was almost independent of gate voltage until the upper well was depleted. We found n_u+n_l to be in good agreement with the total density n_{tot} obtained from Hall measurements. The mobility of the upper well was usually much higher than that of the bottom well, except near resonance or when the upper well was nearly depleted. This results in a relatively large resistivity change at resonance which was advantageous for the present study.

III. CALCULATION OF THERMOPOWER OF A DQW

The thermopower, S, has two components, diffusion, S^d, and phonon drag, S^g, which have different temperature dependencies and so, in principle, they can be separated. We assume that the thermoelectric properties of the DQW can be approximated as two independent 2DEG's connected in parallel. The total thermopower, S, can then be written as

$$S=\frac{\sigma_u S_u+\sigma_l S_l}{\sigma_u+\sigma_l}, \tag{1}$$

where σ is the conductivity and the subscripts u and l denote the upper and the lower layers, respectively.

For a degenerate 2DEG, S^d is given by Mott's expression:[19]

$$S^d=-\frac{\pi^2k_B^2T}{3e\epsilon_F}\left(\frac{\partial\ln\sigma}{\partial\ln\epsilon}\right)_{\epsilon_F}=-\frac{\pi^2k_B^2T}{3e\epsilon_F}(1+p)=AT, \tag{2}$$

where ϵ is the electronic energy, ϵ_F is the Fermi energy, e is the magnitude of the electronic charge, and we assume that the electronic (elastic) relaxation time obeys $\tau^{el}(\epsilon)\propto\epsilon^p$.

The phonon-drag thermopower is calculated within the Cantrell-Butcher framework.[20] This formalism is based on the solution of the coupled Boltzmann equations for electrons and phonons in which two-dimensional (2D) electrons with wave vector $\mathbf{k}=(k_x,k_y)$ are scattered by 3D phonons of wave vector $\mathbf{Q}=(\mathbf{q},q_z)$, where $\mathbf{q}$ is the component of $\mathbf{Q}$ in the plane of the 2DEG. The phonon-drag thermopower of layer i (upper or lower) when only the ground subband is occupied is

$$\begin{aligned}S_i^g=&\frac{-e(2m^*)^{3/2}l_p\tau_i^{el}}{\sigma_i k_B T^2\hbar^4}\frac{V}{(2\pi)^3}\\&\times\sum_s v_p^s\int_0^\infty\int_{-\infty}^\infty dq\,dq_z|U_i(\mathbf{Q}s)|^2N^0_{\mathbf{Q}s}\epsilon_q\\&\times\int_\gamma^\infty d\epsilon_{\mathbf{k}}\frac{f^0(\epsilon_{\mathbf{k}})[1-f^0(\epsilon_{\mathbf{k}}+\hbar\omega_{\mathbf{Q}s})]}{\sqrt{\epsilon_{\mathbf{k}}-\gamma}},\end{aligned} \tag{3}$$

where m^* is the electron band mass, V is the volume of the sample, $\sigma_i=n_ie^2\tau_i^{el}/m^*$ is the conductivity, and l_p is the phonon mean free path. In Eq. (3) we have summed the contributions of the three acoustic branches which are denoted by the polarization index s. We should also mention that a constant elastic relaxation time is assumed, $\tau^{el}(\epsilon_{\mathbf{k}})=\tau^{el}(\epsilon_F)$; previous work suggests[6,21] that this approximation is accurate for degenerate 2DEG's. The frequency of phonons with wave vector $\mathbf{Q}$ and polarization s is $\omega_{\mathbf{Q}s}$ and their phase velocity is v_p^s. $N^0_{\mathbf{Q}}$ is the phonon distribution in equilibrium, $\epsilon_q=\hbar^2q^2/2m^*$, and $\gamma=(\hbar\omega_{\mathbf{Q}}-\epsilon_q)^2/4\epsilon_q$. f^0 is the Fermi-Dirac distribution function and $\epsilon_{\mathbf{k}}=\hbar^2k^2/2m^*$ is the electron energy. Finally, $U_i(\mathbf{Q})$ is the screened e-p potential. Equation (3) is equivalent to the standard expressions used in the literature for the calculation of the phonon-drag thermopower in single quantum wells (see, for example, Refs. 6 and 23).

The expression for the screened e-p interaction is given by

$$U_i(\mathbf{Q}) = U^{bare}(\mathbf{Q}) R_i(q), \tag{4}$$

where $U^{bare}(\mathbf{Q})$ is the Fourier transform of the unscreened e-p potential,[6,20,22]

$$U^{bare}(\mathbf{Q}) = i \Xi^{eff}(\mathbf{Q})(\hbar/2\varrho V \omega_{\mathbf{Q}})^{1/2} Q Z(q_z). \tag{5}$$

Here ϱ is the density of the sample. In GaAs, Ξ^{eff} accounts for both deformation potential and piezoelectric coupling. For the longitudinal branch and for each of the transverse branches $\Xi^{eff}(\mathbf{Q})$ is given by $\{\Xi_d^2 + [(eh_{14})^2 A_l / Q^2]\}^{1/2}$, and $[(eh_{14})^2 A_t / Q^2]^{1/2}$ respectively,[22] where Ξ_d is the deformation potential constant, h_{14} is the piezoelectric constant, and A_l, A_t are the anisotropy factors given by Lyo.[22] Finally, $Z(q_z)$ is a form factor that accounts for the finite thickness of the 2DEG. The expression for $Z(q_z)$ is (see, e.g., Ref. 7)

$$Z(q_z) = \int \phi^2(z) \exp(i q_z z) dz, \tag{6}$$

where $\phi(z)$ is the envelope function in the ground state. By approximating the confining potential by a hard wall potential we take

$$|Z(q_z)|^2 = \frac{2[1-\cos(q_z W)]}{q_z^2 W^2 [(q_z W/2\pi)^2 - 1]^2}, \tag{7}$$

where $W = 18$ nm is the width of each well.

The factor $R_i(q)$ that appears in Eq. (4) introduces screening effects to the e-p coupling. In a single layer $R(q) = 1/\epsilon(q)$ where $\epsilon(q)$ is the static dielectric function.[24,25] Here we take into account the mutual screening of the e-p interaction by electrons in each layer, and $R_i(q)$ is given by[26]

$$R_i(q) = \frac{1 + V_{jj}\Pi_{jj} - V_{ij}\Pi_{ii}}{\epsilon^{intra}(q)}. \tag{8}$$

In Eq. (8) the subscripts i,j denote the layers i and j, respectively, Π_{jj} is the polarization function in the random-phase approximation[24] (RPA), and V_{ij} is the Coulomb interaction given by

$$V_{ij} = \frac{e^2}{2\kappa\kappa_0 q} F_{ij}(q), \tag{9}$$

where κ is the permittivity of GaAs, κ_0 is the permittivity of free space, and $F_{ij}(q)$ are the screening form factors for which we use the form for square wells.[27,28] Finally, $\epsilon^{intra}(q)$ is the intralayer dielectric function (see, e.g., Ref. 28):

$$\epsilon^{intra}(q) = [1 + V_{ii}\Pi_{ii}][1 + V_{jj}\Pi_{jj}] - V_{ij}^2 \Pi_{ii}\Pi_{jj}. \tag{10}$$

We see by inspection that, if we neglect the screening effects of the electrons of the opposite layer, then Eq. (4) becomes $U_i(\mathbf{Q}) = U^{bare}(\mathbf{Q})/\epsilon(q)$ where $\epsilon(q) = 1 + V_{ii}\Pi_{ii}$ is the static dielectric function for a single layer. Then, at low T where $q \ll 2k_F$ (Bloch limit), we obtain the familiar T^4 law for S^g. More specifically, it can be shown that in the Bloch limit we can write[8,9]

$$S^g \propto \frac{l_p T^4}{n^{3/2}}. \tag{11}$$

The full expression and details on the several approximations which lead to the T^4 power law of S^g at low T are given in Ref. 8.

An important result of the present calculations is that the phonon-drag thermopower of a DQW at low temperatures is

$$S^g \propto \frac{l_p T^5}{n^{\alpha}} \tag{12}$$

with

$$\alpha \approx 2$$

instead of the standard result in Eq. (11). Note that Eq. (12) is a numerical result which has been tested in the Bloch limit for the lowest temperatures of interest here ($0.2 < T < 0.4$ K) and for all the measured densities of the upper layer ($0.26 < n_u < 1.4 \times 10^{15}$ m^{-2}). It does not seem to be possible to derive an analytic approximation for S_i^g of the layer i at low T in the case of a DQW because the factor $R_i(q)$ [Eq. (8)] which describes the screening effects is a complicated function of q, k_{Fi}, and d. However, the difference from the standard T^4 power law is due to the mutual screening of the e-p coupling by electrons in each layer and, in order to understand the origin of this difference, we compare the behavior of the dielectric factors $R(q)$ and $R_i(q)$ for a single layer and a DQW system, respectively, at low temperatures. In a single layer the dielectric function at low temperatures is $\epsilon(q) \approx Q_s/q$,[8,23] where $Q_s = e^2 m^*/(2\pi\hbar^2\kappa\kappa_0)$. Consequently, $R(q) \approx q/Q_s \propto T$. By inspection of Eq. (8) we see that at low temperatures $R_i(q) \approx q/\{Q_s[1+\exp(-qd)]\}$. This simple result is obtained by assuming that the screening form factors F_{11} and F_{22} are unity and $F_{12} \approx \exp(-qd)$ when $T \to 0$ (see Ref. 27). Moreover, in the static, long-wavelength limit, the polarization functions are $\Pi_{11} \approx \Pi_{22} \approx \Pi_{12} \approx m^*/\pi\hbar^2$. The factor $1/[1+\exp(-qd)]$ is an increasing function of T which explains the stronger temperature dependence of S_i^g in a DQW. At the lowest temperatures examined here the product qd is of the order of unity. We see by inspection that when the center-to-center distance of the two layers is large ($qd \gg 1$) the theoretical values of S_i^g become identical to those of a single layer and will show a T^4 dependence at low T. Also, at very low temperatures ($T < 20$ mK) we should again obtain a T^4 power law, but now the calculated values of S_i^g are smaller by a factor of 4 than those of a single layer.

Another important point we should make here is that the RPA gives a good description of the dielectric properties of an interacting electron gas in the high-density limit ($r_s < 1$, where r_s is the RPA parameter). However, the carrier densities considered here are relatively low and for this reason it is necessary to take into account the local-field correction

(LFC) to the RPA due to the effects of exchange and correlation.[10] The RPA parameter for 2DEG's is[29] $r_s = 1/(\alpha^{*2}\pi n)^{1/2}$ where α^* is the effective Bohr radius which is 10.3 nm for GaAs. For the densities of interest here $1.4 < r_s < 4$. The LFC is incorporated in our calculations by writing the intralayer Coulomb potential V_{ii} as

$$V_{ii} = \frac{e^2}{2\kappa\kappa_0 q}[1 - G(q)]F_{ii}(q), \tag{13}$$

where $G(q)$ is given by Gold and Calmels:[10]

$$G(x) = r_s^{2/3}\frac{1.402x}{[2.644C_{12}^2 + x^2C_{22}^2]^{1/2}} \tag{14}$$

with $x = q/q_0$, $q_0 = 2/(r_s^{2/3}\alpha^*)$, $C_{12} = 1.914r_s^{0.119}$, and $C_{22} = 1.640r_s^{0.530}$.

The LFC to the RPA leads to a significant increase of the calculated values of S_u^g at low densities for the upper layer (recall that this layer depleted to zero density in these experiments). However, the inclusion of the LFC does not significantly affect the T dependence of S^g. Recently, Pillarisetty *et al.*[30] observed a strong enhancement of the drag resistivity of dilute hole double-layer systems in the regime of $r_s = 19 - 39$. In addition they observed deviations from the standard T^2 dependence expected from Boltzmann calculations[28] which were not related to phonon-mediated, plasmon-enhanced, or disorder-related mechanisms (see Ref. 30, and references therein). Our present analysis suggests that the LFC to the static dielectric function could lead to significant effects to the drag calculations in dilute gases and it should be taken into account. The effect is expected to be stronger in hole gases because the short-range correlations are more pronounced due to the higher effective mass of holes.[31]

We should mention here that the picture of the two independent quantum wells is an approximation to the real system and ignores interwell coupling. The approximation is valid when $k_F d \gg 1$ where k_F is the Fermi wave number and d is the center-to-center distance between the 2DEG's, and for our sample we find that $k_F d \approx 1.5$ when $n_u = n_l$. Therefore, it is essential to carry out a full self-consistent calculation of S^g at resonance to make sure that one does indeed find essentially the same result as with two independent wells. Such a calculation is described in the Appendix. The results of the two sets of calculations are in good agreement, which strongly supports the validity of our approximation.

IV. RESULTS

The resistivity was measured at various temperatures as a function of gate voltage, but Fig. 1 shows only the data at 0.3 K. The resonance is clearly seen at $n_{tot} \approx 1.72 \times 10^{15}$ m^{-2} ($V_g \approx -0.04$ V) so that $n_u \approx n_l \approx 0.86 \times 10^{15}$ m^{-2} at this point. The solid line is the estimated behavior if there was no tunneling between the layers. As seen in previous work, the resonance broadens as the temperature increases.[2] Over most of the figure the resistivity is dominated by the high-mobility upper layer, except near resonance (where the mobilities become equal due to tunneling) and near total depletion of the upper layer. The small kink in the resistivity near $n_{tot} = 1.1 \times 10^{15}$ m^{-2} ($V_g \approx -0.34$ V) corresponds to the region where the conductivities of the layers are approximately the same. The upper layer becomes fully depleted at $V_g \approx -0.46$ V.

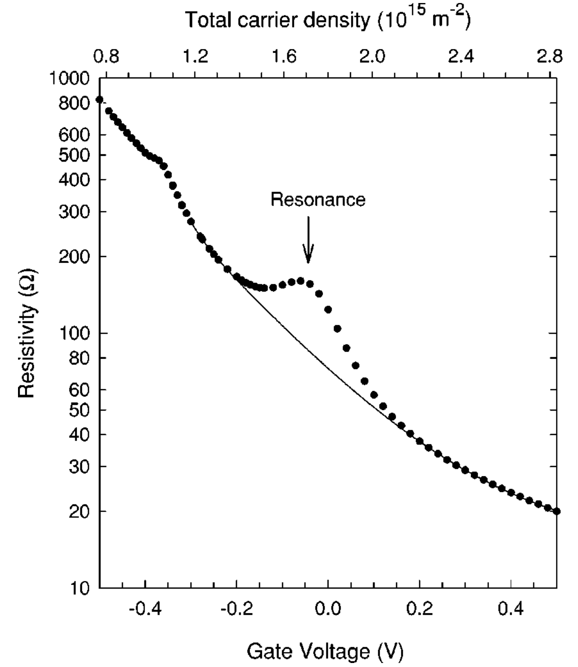

FIG. 1. The resistivity as a function of gate voltage and total electronic density showing the resonance. The small kink in the curve at low densities is caused by the conductivities of the two wells becoming similar.

We measured S as a function T at ten different gate voltages. In Fig. 2 we present the experimental values of S/λ for $n_u = 1.47$, 1.66, 1.80, and 2.21×10^{15} m^{-2}. Plotting the data like this is useful for a number of reasons. First, over most of the temperature range S^g is dominant and varies rapidly with temperature. Using S/λ eliminates most of the dependence. Second, S^g and λ are each proportional to the phonon mean free path, l_p, so their ratio becomes independent of l_p and closer to being a quantity independent of the particular substrate dimensions and properties. Finally, this quantity does not require the measurement of the temperature gradient so the random errors should be somewhat smaller than for S.

The low-temperature parts of these curves were analyzed assuming $S/\lambda = A'/T^2 + BT^m$ where $m = 1$ or 2 depending on whether Eq. (11) or Eq. (12) is appropriate. The constant A' arises from diffusion and is related in a simple way to A in Eq. (2). This analysis could not definitively distinguish between the two possibilities, mainly because the density of the wells is typically so low that the temperature required for Eqs. (11) and (12) to be valid is often $\lesssim 0.4$ K and this is where S^d (which is proportional to T) becomes dominant. Indeed, for two of the data sets taken with the upper layer almost totally depleted, neither form represents the data satisfactorily which probably results from the upper well density being so low that the low temperature requirement was not reached.

When the remaining eight data sets' data were analyzed

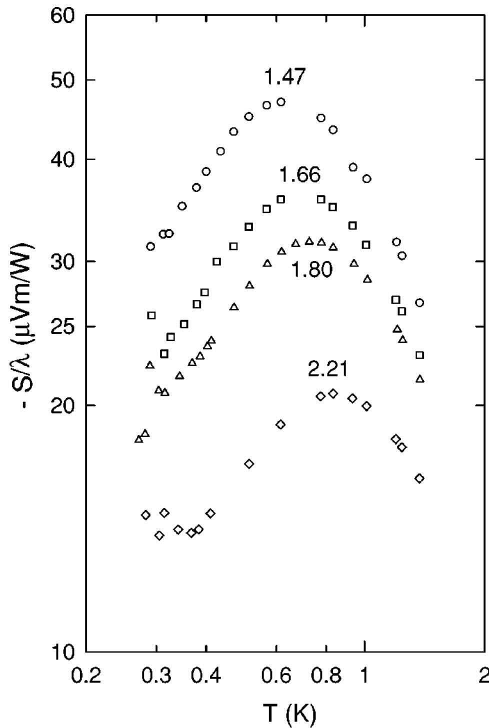

FIG. 2. The experimental values of S/λ as a function of T. The values on the curves are the total electronic densities in units of $10^{15}\ \mathrm{m}^{-2}$. The symbols are ○, $1.47\times10^{15}\ \mathrm{m}^{-2}$ ($V_g=-0.16$ V); □ $1.66\times10^{15}\ \mathrm{m}^{-2}$ ($V_g=-0.07$ V); △, $1.80\times10^{15}\ \mathrm{m}^{-2}$ ($V_g=0.00$ V); and ◇, $2.21\times10^{15}\ \mathrm{m}^{-2}$ ($V_g=0.20$ V).

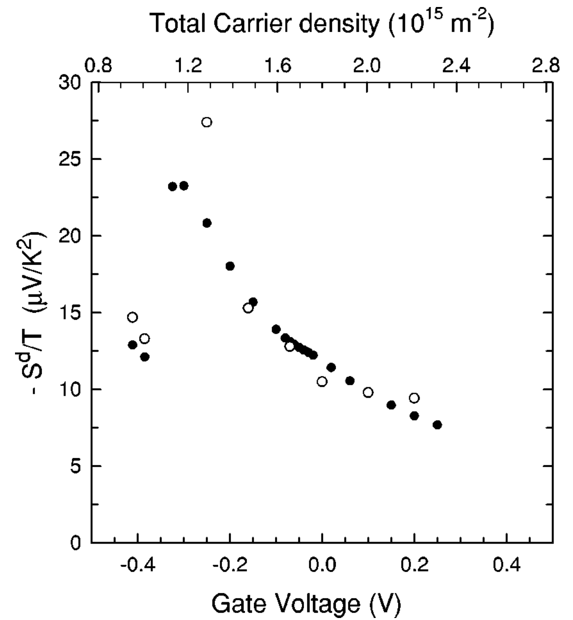

FIG. 3. The coefficient of the diffusion thermopower $A=S^d/T$ as a function of gate voltage and total carrier density. Experimental values of A are shown as open circles. The solid circles are the calculated values assuming that the scattering coefficient $p=0.5$ is the same for both wells and is independent of density.

using $m=1$, S^d was found to have almost no dependence on V_g, a very unexpected result and unlikely to be correct. On the other hand the use of $m=2$ as predicted by theory leads to a behavior for S^d in keeping with expectations. Because of this, only results for $m=2$ are shown here. The values deduced for $A=S^d/T$ are shown in Fig. 3 as a function of V_g (open circles). In the same figure we also present the calculated values of S^d/T obtained using Eqs. (1) and (2) with $p=0.5$ (solid circles). This value of p was chosen to fit the data in the midrange.

The simple theory fits the data surprisingly well, perhaps fortuitously so. If p had been significantly different for the two wells we would have expected to see a reflection of the resonance in S^d. Over most of the range the upper well dominates Eq. (1) because of its high conductivity, and the rise in S^d/T is due to the decreasing number of carriers as V_g decreases. However, near resonance the wells contribute equally so there would be a peak or trough around the resonance position if p had a different value in each well. It is also possible that p might depend on layer density and this may be responsible for the discrepancy seen just before the upper well completely depletes.

If the diffusion term A'/T^2 is subtracted from the data in Fig. 2 we obtain data on S^g/λ which are plotted in Fig. 4 as symbols. For comparison, S^g has been evaluated numerically using Eqs. (1)–(14) and the standard parameters for GaAs.[7,6] To eliminate l_p we have made use of the lattice thermal conductivity λ which is predicted to be $\lambda=3.89 l_p T^3$ for a GaAs substrate at low temperatures,[8] with l_p in mm. The calculated results for S^g/λ are shown in Fig. 4 as solid lines. We find that the theoretical values of S^g have a very similar T dependence to the experimental values, but are always higher by about 25%. This difference could be due simply to the uncertainties in various constants required in the calculations and experiments (e.g., average velocities and experimental dimensions).

Figure 5 shows experimental results for S^g (open symbols) plotted in the form $S^g/\lambda T^2$ as a function of V_g at two fixed temperatures of 0.30 K and 0.41 K. In order to obtain more points for this curve, S was measured at many gate voltages at these two temperatures. We then subtracted S^d using interpolated values from the experimental data shown in Fig. 3; this curve is not well defined in the region of the peak but fortunately this is where S^g becomes very large so the resulting errors remain relatively small. According to Eq. (12), $S^g/\lambda T^2$ should be independent of T in the low-temperature limit, and indeed the two curves appear to be coincident over most of the range. However, near the peak in Fig. 5 the upper well has a very low density and the low-temperature requirements are not satisfied, so that $S^g/\lambda T^2$ depends on T in this region.

Again, for comparison, S^g has been evaluated numerically and the results are shown in Fig. 5 as solid symbols. The agreement between experiment and theory is generally very good. We should mention that, because S^g is mainly determined by the upper well, small absolute errors in n_u become very significant when the well is almost depleted (around the peak in Fig. 5). We believe the small discrepancy in the peak positions of the experimental and theoretical curves is largely due to this. The calculation of S^g as a function of density of the upper layer provides useful information about the impor-

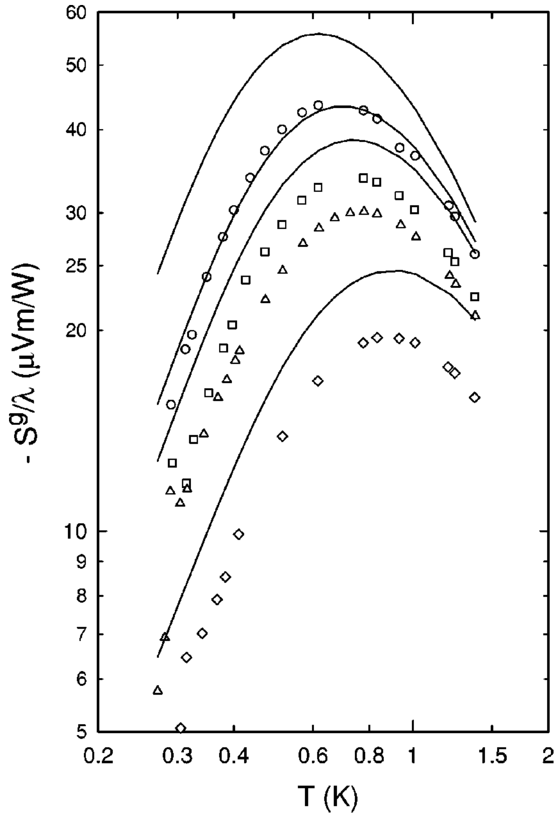

FIG. 4. The ratio S^g/λ, for both experiment (symbols) and calculation (lines). The experimental data are obtained by subtracting the diffusion component from the data in Fig. 2, as a function of T. The meaning of the symbols is the same as in Fig. 2. The calculated lines are for the same total densities and are in the same order (top to bottom) as the experimental data, i.e., $n = 1.47\times10^{15}$ m^{-2}, 1.66×10^{15} m^{-2}, 1.80×10^{15} m^{-2}, and 2.21×10^{15} m^{-2}. All the lines approach T^2 at the lowest temperatures.

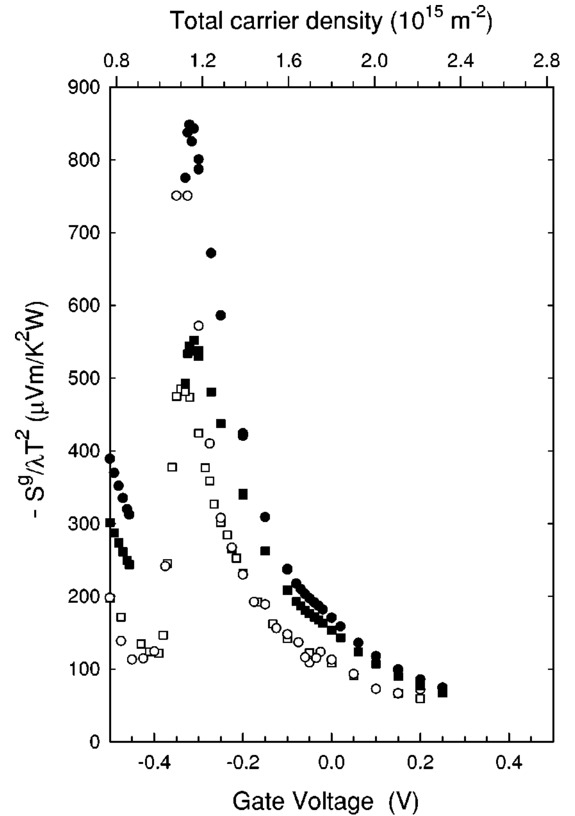

FIG. 5. The calculated results for $S^g/\lambda T^2$ as a function of gate voltage and carrier density. The open symbols are the experimental points and the solid symbols are the calculated values. The circles correspond to 0.30 K and the squares to 0.41 K.

tance of the LFC factor $G(q)$ appearing in Eq. (13). At $n_u = 0.26\times10^{15}$ m^{-2}, which is the lowest value of density examined, we find that S_u^g calculated using Eqs. (13) and (14) instead of Eq. (9) is increased by a factor of 2.5. This is in good agreement with the experimental results near the peak of $S^g/\lambda T^2$ in Fig. 5. At high densities ($r_s \approx 1$) the effect of the LFC is much less pronounced.

Finally we note that when the upper well is empty, Eq. (11) becomes appropriate so that $S^g/\lambda T^2$ does not become constant as $T\rightarrow 0$. However, we have included these data on the plot so that the strong effect of the total depletion of the upper well can be seen.

V. DISCUSSION

In contrast to the behavior of resistivity, there is no obvious effect on either component of the thermopower as the DQW is taken through resonance. The model of two independent wells should certainly be appropriate well away from resonance. The fact that the model works so well even at resonance is surprising and this is one of the main points of interest in this section. We discuss each component separately.

Although S^g shows a strong dependence on V_g, there is no superimposed resonance analogous to that in resistivity. Both of these features are reproduced by the calculations assuming uncoupled wells. As we have shown in the Appendix, a full calculation of S^g at the resonance gives almost the same result as for two independent wells, which adds strong support for the model. The lack of any feature around the resonance position seems to result mainly from the fact that S^g is independent of impurity scattering of the electrons.[6] The main effect of the resonance on the electron properties is to average the impurity scattering in each well, but phonon scattering is independent of mobility and is primarily determined by the densities of electrons in the wells [cf. Eqs. (11) and (12)]. Away from resonance the high-mobility upper well dominates the resultant S^g [via Eq. (1)] and the rise in $S^g/\lambda T^2$ as V_g is decreased seen in Fig. 5 is due to the decrease in n_u. Interestingly, at resonance both wells have the same conductivity so that they contribute equally to the resultant S^g [again, see Eq. (1)], but they also have identical S_i^g and so their resultant S^g is the same as if the upper well still acted alone.

The numerical calculations show that for $V_g < -0.17$ V the contribution of the lower layer starts to give a noticeable contribution to S^g due to the decreasing number of carriers in the top layer. Finally, around -0.34 V the conductivities of both layers become equal and S^g is just the average of S_u^g and S_l^g. This corresponds to the peak observed in $S^g/\lambda T^2$. Below

this value of n_u the contribution of the lower layer becomes dominant causing a significant decrease of S since n_l is now larger than n_u. Finally, when the upper layer becomes fully depleted ($V_g = -0.46$ V) S^g again increases as V_g decreases due to the decrease of n_l.

As with resistivity, diffusion thermopower is controlled by impurity scattering in the temperature region of interest, so it seems likely that the resonance would be reflected in this coefficient. In view of Eq. (2), one might initially have expected S^d to resemble the derivative of resistivity with gate voltage V_g (cf. Fig. 1). However, the effect of varying V_g is to change the density of the electrons in the top well leaving the bottom well almost unchanged. This changes ϵ_F only for the top well (relative to the bottom of the well) and allows resonance to be achieved in this system. This is quite different from varying the energy of both wells simultaneously as Eq. (2) requires at any particular fixed value of V_g. In this case the system is not swept through resonance by varying ϵ. A full calculation would be needed to confirm that this explanation is quantitatively correct.

As we have noted earlier, if the partial diffusion thermopowers for each well happen to have the same magnitudes as a function of density [i.e., the factor $p = (\partial \ln \tau / \partial \ln \epsilon)_{\epsilon_F}$ is the same] then the total thermopower given by Eq. (1) will not show a resonance. This will presumably remain valid even when the two wells are strongly coupled and the electrons spend equal time in the two states. The fact that both wells seem to have a similar value of p might be partly coincidental in the present case where the two wells have very different mobilities. Perhaps other DQW's will show some sensitivity to the resonance.

VI. CONCLUSIONS

In general the theoretical and experimental results on all aspects of the thermopower in a double quantum well are in excellent agreement. The data on phonon-drag thermopower as a function of gate voltage at two fixed temperatures of $T = 0.30$ K and 0.41 K are particularly interesting. First, they reveal that phonon-drag thermopower does not show any resonance structure and, second, they have allowed us to investigate the role of the local-field correction to the static dielectric function in dilute 2DEG's. A considerable amount of theoretical work has focused on the dielectric properties of dilute gases when the RPA is no longer accurate due to exchange and correlation effects. Our experiments provide clear evidence for the importance of the LFC at low densities.

ACKNOWLEDGMENTS

The work was supported by the Natural Sciences and Engineering Research Council of Canada. We also thank Dr. Jean Beerens of the University of Sherbrooke for help with samples.

APPENDIX: CALCULATION OF THE PHONON-DRAG THERMOPOWER OF TWO COUPLED SYMMETRIC QUANTUM WELLS

In this Appendix we outline a calculation of S^g for two coupled symmetric quantum wells. The parameters correspond to the present case, i.e., width 18 nm each, barrier height 228 meV, and separation 3.4 nm. We consider only the two lowest subbands, the so-called symmetric and antisymmetric, with energies $\epsilon_1 = 12.02$ meV and $\epsilon_2 = 12.91$ meV, respectively. The electron density in each well is $n_i = (m^*/\pi\hbar^2)(\epsilon_F - \epsilon_i)$, with $i = 1,2$, respectively, giving $n_1 = 0.986 \times 10^{15}$ m^{-2}, $n_2 = 0.735 \times 10^{15}$ m^{-2}, and corresponding Fermi wave numbers of $k_{F1} = 0.079$ nm^{-1}, $k_{F2} = 0.068$ nm^{-1}.

The phonon-drag thermopower in the two-subband quantum well system is given by[20]

$$S^g = -\sum_{i,j} L_{ij}/\sigma, \tag{A1}$$

where $i,j = 1,2$; σ is the total conductivity $\sigma = \sigma_1 + \sigma_2$ with $\sigma_i = n_i e^2 \tau_i^{el}/m^*$, and L_{ij} are the thermoelectric coefficients $L = J_x/E_x$, where J_x is the thermoelectric current in the x direction and E_x is the associated electric field. The subscript ij denotes $i \to j$ transitions. The expressions for L_{ij} are given by Cantrell and Butcher,[20]

$$L_{ij} = -\frac{e\tau_p \tau_i^{el}}{A k_B T^2} \sum_{\mathbf{Q}} \sum_{\mathbf{k}} \sum_{\mathbf{k}'} \hbar\omega_{\mathbf{Q}} \mathbf{v}_p \cdot \mathbf{v}(\mathbf{k}) \{ f_i^0(\epsilon_{\mathbf{k}})[1 - f_j^0(\epsilon_{\mathbf{k}'})] P_{ij}^a(\mathbf{k},\mathbf{k}') - f_j^0(\epsilon_{\mathbf{k}'})[1 - f_i^0(\epsilon_{\mathbf{k}})] P_{ji}^a(\mathbf{k}',\mathbf{k}) \}, \tag{A2}$$

where τ_p is the phonon relaxation time, $f_i^0(\epsilon_{\mathbf{k}}) = [\exp(\epsilon_{i\mathbf{k}} - \epsilon_F/k_B T) + 1]^{-1}$ is the Fermi-Dirac distribution function for the i subband and $\epsilon_{i\mathbf{k}} = \epsilon_i + \epsilon_{\mathbf{k}}$, with $\epsilon_{\mathbf{k}} = \hbar^2 k^2/2m^*$, is the corresponding electron energy. Finally, $P_{ij}^a(\mathbf{k},\mathbf{k}')$ is the rate at which an electron will transfer from $i\mathbf{k}$ to $j\mathbf{k}'$ by absorbing one phonon with wave vector $\mathbf{Q}$ when the whole system is in thermal equilibrium. The expression for $P_{ij}^a(\mathbf{k},\mathbf{k}')$ is given by[6,20]

$$P_{ij}^a(\mathbf{k},\mathbf{k}') = \frac{2\pi}{\hbar} N_{\mathbf{Q}}^0 |U_{ij}(\mathbf{Q})|^2 \delta(\epsilon_{j\mathbf{k}'} - \epsilon_{i\mathbf{k}} - \hbar\omega_{\mathbf{Q}}) \delta_{\mathbf{k}',\mathbf{k}+\mathbf{q}}, \tag{A3}$$

where N_Q^0 is the phonon distribution in equilibrium. $U_{ij}(\mathbf{Q})$ is the effective screened potential given by[32]

$$U_{ij}(\mathbf{Q}) = \sum_{kl} U_{kl}^{bare}(\mathbf{Q}) \epsilon_{klij}^{-1}(q), \tag{A4}$$

where $U_{kl}^{bare}(\mathbf{Q})$ is the Fourier transform of the unscreened e-p absorption potential given by

$$U_{ij}^{bare}(\mathbf{Q}) = i\Xi_{eff}(\hbar/2\varrho V\omega_{\mathbf{Q}})^{1/2} Q Z_{ij}(q_z). \tag{A5}$$

Here ϱ and V are the density and the volume of the material and $\phi_i(z)$ is the electron envelope wave function which corresponds to the energy level ϵ_i. The form factor $Z_{ij}(q_z)$ is given by

$$Z_{ij}(q_z) = \int \phi_i(z)\phi_j(z)\exp(iq_z z)dz. \tag{A6}$$

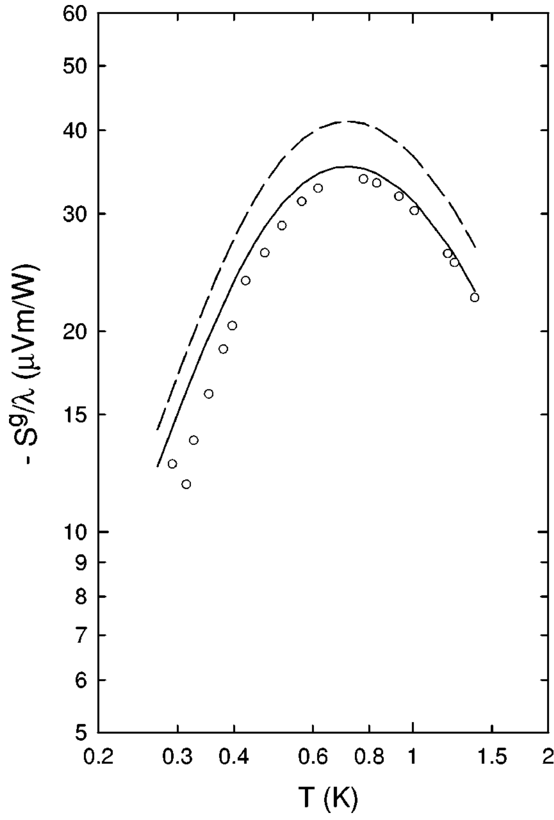

FIG. 6. Comparison of the calculated S^g/λ at resonance for the coupled (solid line) and uncoupled (dashed line) wells. The open circles represent the experimental data.

In Eq. (A4) $\epsilon_{klij}^{-1}(q)$ are the components of the inverse dielectric matrix given by[25,26]

$$\epsilon_{klij}(q)=\delta_{ki}\delta_{lj}-V_{klij}(q)\Pi_{ij}, \tag{A7}$$

where Π_{ij} is the polarization function[25,32] and $V_{klij}(q)$ is the 2D Fourier transform of the Coulomb interaction given by

$$V_{klij}(q)=\frac{e^2}{2\kappa\kappa_0 q}F_{klij}(q), \tag{A8}$$

where κ is the permittivity of GaAs, κ_0 is the permittivity of free space, and

$$F_{klij}(q)=\int dz\int dz'\,\phi_k(z)\phi_l(z)\times\exp(-q|z-z'|)\phi_i(z')\phi_j(z'). \tag{A9}$$

For the symmetric double quantum well system we consider here Eq. (A9) imposes the following symmetry relationships: $V_{klij}=0$ if $k+l+i+j$ is odd and $V_{1212}=V_{2112}=V_{2121}=V_{1221}$, $V_{1122}=V_{2211}$.

In Eq. (A2) the summation over $\mathbf{k}'$ is carried out straightforwardly by replacing $\mathbf{k}'$ by $\mathbf{k}+\mathbf{q}$ and $\mathbf{k}-\mathbf{q}$ in the terms proportional to $P_{ij}^a(\mathbf{k},\mathbf{k}')$ and $P_{ji}^a(\mathbf{k}',\mathbf{k})$, respectively. Moreover, we make use of the energy conservation condition imposed by the δ function appearing in the transition rates $P_{ij}^a(\mathbf{k},\mathbf{k}')$ and $P_{ji}^a(\mathbf{k}',\mathbf{k})$. Then we take

$$L_{ij}=-\frac{e\hbar l_p\tau_i^{el}}{m^*Ak_BT^2}\sum_{\mathbf{Q}}\sum_{\mathbf{k}}\hbar\,v_p\mathbf{q}\cdot\mathbf{k}\{f_i^0(\epsilon_{\mathbf{k}})\times[1-f_i^0(\epsilon_{\mathbf{k}}+\hbar\omega_{\mathbf{Q}})]P_{ij}^a(\mathbf{k},\mathbf{k}+\mathbf{q})-f_i^0(\epsilon_{\mathbf{k}}-\hbar\omega_{\mathbf{Q}})[1-f_i^0(\epsilon_{\mathbf{k}})]P_{ji}^a(\mathbf{k}-\mathbf{q},\mathbf{k})\}, \tag{A10}$$

where in Eq. (A10) the product $\mathbf{v}_p\cdot\mathbf{v}(\mathbf{k})$ is replaced by $(\hbar v_p/m^*)(\mathbf{q}\cdot\mathbf{k}/Q)$ and $l_p=v_p\tau_p$ is the phonon mean free path. The expressions for the transition rates $P_{ij}^a(\mathbf{k},\mathbf{k}+\mathbf{q})$ and $P_{ji}^a(\mathbf{k}-\mathbf{q},\mathbf{k})$ are

$$P_{ij}^a(\mathbf{k},\mathbf{k}+\mathbf{q})=\frac{2\pi}{\hbar}N_{\mathbf{Q}}^0|U_{ij}(\mathbf{Q})|^2\times\delta\left(\Delta_{ji}+\epsilon_q+\frac{\hbar^2}{m^*}\mathbf{k}\cdot\mathbf{q}-\hbar\omega_{\mathbf{Q}}\right), \tag{A11}$$

$$P_{ji}^a(\mathbf{k}-\mathbf{q},\mathbf{k})=\frac{2\pi}{\hbar}N_{\mathbf{Q}}^0|U_{ij}(\mathbf{Q})|^2\times\delta\left(-\Delta_{ji}-\epsilon_q+\frac{\hbar^2}{m^*}\mathbf{k}\cdot\mathbf{q}-\hbar\omega_{\mathbf{Q}}\right). \tag{A12}$$

In Eqs. (A11) and (A12) $\Delta_{ji}=\epsilon_j-\epsilon_i$ and $\epsilon_q=\hbar^2q^2/2m^*$. By inspection of Eqs. (A11) and (A12) we see that the product $\mathbf{q}\cdot\mathbf{k}$ in Eq. (A10) can be replaced by $[\hbar\omega_{\mathbf{Q}}-(\Delta_{ji}+\epsilon_q)]m^*/\hbar^2$ and $[\hbar\omega_{\mathbf{Q}}+(\Delta_{ji}+\epsilon_q)]m^*/\hbar^2$ when it multiplies $P_{ij}^a(\mathbf{k},\mathbf{k}+\mathbf{q})$ and $P_{ji}^a(\mathbf{k}-\mathbf{q},\mathbf{k})$, respectively.

By expressing $\mathbf{k}$ in polar coordinates $\mathbf{k}=(k\cos\theta,k\sin\theta)$ and $\mathbf{Q}$ in cylindrical coordinates $\mathbf{Q}=(q\cos\phi,q\sin\phi,q_z)$ we can replace the summations over $\mathbf{k}$ and $\mathbf{Q}$ by

$$\sum_{\mathbf{k}}\rightarrow\frac{A}{2\pi}\int k\,dk=\frac{Am^*}{2\pi\hbar^2}\int d\epsilon_{\mathbf{k}}, \tag{A13}$$

$$\sum_{\mathbf{Q}}\rightarrow\frac{V}{(2\pi)^3}\int_0^\infty\int_{-\infty}^\infty\int_0^{2\pi}q\,dq\,dq_z d\phi. \tag{A14}$$

We see by inspection that the angle ϕ occurs in the arguments of the δ functions in Eqs. (A11) and (A12). Thus the integration over ϕ is carried out straightforwardly as

$$\int_0^{2\pi}\delta\left[\pm(\Delta_{ji}+\epsilon_q)+\frac{\hbar^2kq}{m^*}\cos\phi-\hbar\omega_{\mathbf{Q}}\right]d\phi=\frac{\epsilon_q^{-1/2}}{\sqrt{\epsilon_{\mathbf{k}}-\gamma_{ji}^{\mp}}}, \tag{A15}$$

where $\gamma_{ji}^{\pm}=[\hbar\omega_{\mathbf{Q}}\pm(\epsilon_q+\Delta_{ji})]^2/4\epsilon_q$.

By substituting Eqs. (A11)–(A15) into Eq. (A10) we take

$$L_{ij}=-\frac{e(2m^*)^{3/2}l_p\tau^{el}}{2k_BT^2\hbar^4}\frac{V}{(2\pi)^3}\sum_s v_p^s\int_0^\infty\int_{-\infty}^\infty dq\,dq_zN^0_{\mathbf{Q}s}|U_{ij}(\mathbf{Q}s)|^2$$
$$\times\left\{(\hbar\omega_{\mathbf{Q}s}-\Delta_{ji}-\epsilon_q)\int_{\gamma_{ji}^-}^\infty d\epsilon_{\mathbf{k}}\frac{f_i^0(\epsilon_{\mathbf{k}})[1-f_i^0(\epsilon_{\mathbf{k}}+\hbar\omega_{\mathbf{Q}s})]}{\sqrt{\epsilon_{\mathbf{k}}-\gamma_{ji}^-}}-(\hbar\omega_{\mathbf{Q}s}+\Delta_{ji}+\epsilon_q)\int_{\gamma_{ji}^+}^\infty d\epsilon_{\mathbf{k}}\frac{f_i^0(\epsilon_{\mathbf{k}}-\hbar\omega_{\mathbf{Q}s})[1-f_i^0(\epsilon_{\mathbf{k}})]}{\sqrt{\epsilon_{\mathbf{k}}-\gamma_{ji}^+}}\right\},\tag{A16}$$

where in the above equation we have added the contributions from the three acoustic branches. For the purposes of our analysis we write the second integral in Eq. (A16) in a more convenient form using the identity $f_i^0(\epsilon_{\mathbf{k}})=f_j^0(\epsilon_{\mathbf{k}}-\Delta_{ji})$. Moreover, by changing the integration variable from $\epsilon_{\mathbf{k}}$ to $\epsilon_{\mathbf{k}}+\hbar\omega_{\mathbf{Q}}+\Delta_{ji}$ we see by inspection that

$$\int_{\gamma_{ji}^+}^\infty d\epsilon_{\mathbf{k}}\frac{f_i^0(\epsilon_{\mathbf{k}}-\hbar\omega_{\mathbf{Q}s})[1-f_i^0(\epsilon_{\mathbf{k}})]}{\sqrt{\epsilon_{\mathbf{k}}-\gamma_{ji}^+}}=\int_{\gamma_{ij}^-}^\infty d\epsilon_{\mathbf{k}}\frac{f_j^0(\epsilon_{\mathbf{k}})[1-f_j^0(\epsilon_{\mathbf{k}}+\hbar\omega_{\mathbf{Q}})]}{\sqrt{\epsilon_{\mathbf{k}}-\gamma_{ij}^-}},\tag{A17}$$

where $\gamma_{ij}^-=(\hbar\omega_{\mathbf{Q}}-\epsilon_q-\Delta_{ij})^2/4\epsilon_q$. Then Eq. (A16) is readily written as

$$L_{ij}=-\frac{e(2m^*)^{3/2}l_p\tau^{el}}{2k_BT^2\hbar^4}\frac{V}{(2\pi)^3}\sum_s v_p^s\int_0^\infty\int_{-\infty}^\infty dq\,dq_zN^0_{\mathbf{Q}s}|U_{ij}(\mathbf{Q}s)|^2$$
$$\times\left\{(\hbar\omega_{\mathbf{Q}s}-\Delta_{ji}-\epsilon_q)\int_{\gamma_{ji}^-}^\infty d\epsilon_{\mathbf{k}}\frac{f_i^0(\epsilon_{\mathbf{k}})[1-f_i^0(\epsilon_{\mathbf{k}}+\hbar\omega_{\mathbf{Q}s})]}{\sqrt{\epsilon_{\mathbf{k}}-\gamma_{ji}^-}}-(\hbar\omega_{\mathbf{Q}s}+\Delta_{ji}+\epsilon_q)\int_{\gamma_{ij}^-}^\infty d\epsilon_{\mathbf{k}}\frac{f_j^0(\epsilon_{\mathbf{k}})[1-f_j^0(\epsilon_{\mathbf{k}}+\hbar\omega_{\mathbf{Q}s})]}{\sqrt{\epsilon_{\mathbf{k}}-\gamma_{ij}^-}}\right\}.\tag{A18}$$

We have calculated S^g using Eqs. (A1) and (A18) and the standard parameters for GaAs.[7,6] The results for the ratio S^g/λ are shown by the solid line in Fig. 6. In the same figure we also show the values of S^g/λ calculated by assuming two independent 2DEG's with sheet densities $n_u=n_l=0.86\times10^{15}\ \mathrm{m}^{-2}$ (dashed line). Considering the wells as coupled, the calculated values of S^g are approximately 15% lower for all T compared to those obtained by treating them as uncoupled. The very good agreement between these two calculations justifies the assumption of two uncoupled quantum wells made in the main text. In Fig. 6 we also present the experimental values of S^g/λ for $n_u=0.86\times10^{15}\ \mathrm{m}^{-2}$. The theoretical estimation of S^g by assuming coupled wells is actually in better agreement with the experiment, but we should not read too much into this. There are various constants required in the experimental data (in particular, the geometric dimensions) and theory (e.g., the averages of the sound velocities) which lead to uncertainties similar to the observed differences.

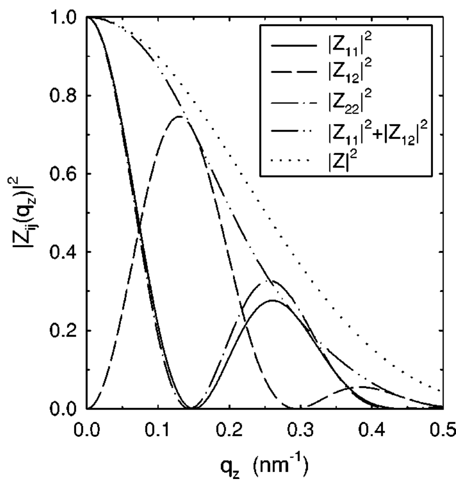

FIG. 7. The form factors $|Z_{ij}(q_z)|^2$ obtained from Eq. (A6) for the case of two coupled wells of width 18 nm. An interesting point in our analysis is the similarity of the sum $|Z_{11}(q_z)|^2+|Z_{12}(q_z)|^2$ (dash-dot-dotted line) and the form factor $|Z(q_z)|^2$ (dotted line) of a single well of width 18 nm obtained from Eq. (7).

In order to obtain physical insight into the similarity of the calculated values of S^g appearing in Fig. 6 we return to Eq. (A18) and examine the contribution of the intrasubband $i\rightarrow i$ and intersubband $i\rightarrow j$ transitions to the thermoelectric coefficient L. It can easily be shown that

$$L_{ii}=\frac{e(2m^*)^{3/2}l_p\tau^{el}}{k_BT^2\hbar^4}\frac{V}{(2\pi)^3}\times\sum_s v_p^s\int_0^\infty\int_{-\infty}^\infty dq\,dq_zN^0_{\mathbf{Q}s}|U_{ii}(\mathbf{Q}s)|^2\epsilon_q\times\int_\gamma^\infty d\epsilon_{\mathbf{k}}\frac{f_i^0(\epsilon_{\mathbf{k}})[1-f_i^0(\epsilon_{\mathbf{k}}+\hbar\omega_{\mathbf{Q}s})]}{\sqrt{\epsilon_{\mathbf{k}}-\gamma}}.\tag{A19}$$

Moreover the sum of the intersubband contributions $i\rightarrow j$ and $j\rightarrow i$ to L is

$$L_{ij}+L_{ji}=\frac{e(2m^*)^{3/2}l_p\tau^{el}}{k_BT^2\hbar^4}\frac{V}{(2\pi)^3}\times\sum_s v_p^s\int_0^\infty\int_{-\infty}^\infty dq\,dq_zN^0_{\mathbf{Q}s}|U_{ij}(\mathbf{Q}s)|^2\epsilon_q\times\left\{\int_{\gamma_{ji}^-}^\infty d\epsilon_{\mathbf{k}}\frac{f_i^0(\epsilon_{\mathbf{k}})[1-f_i^0(\epsilon_{\mathbf{k}}+\hbar\omega_{\mathbf{Q}s})]}{\sqrt{\epsilon_{\mathbf{k}}-\gamma_{ji}^-}}+\int_{\gamma_{ij}^-}^\infty d\epsilon_{\mathbf{k}}\frac{f_j^0(\epsilon_{\mathbf{k}})[1-f_j^0(\epsilon_{\mathbf{k}}+\hbar\omega_{\mathbf{Q}s})]}{\sqrt{\epsilon_{\mathbf{k}}-\gamma_{ij}^-}}\right\}. \quad \text{(A20)}$$

In order to compare the integrals appearing into Eqs. (A19) and (A20) we make the approximations $\gamma_{ij}^-\approx\gamma_{ji}^-\approx\gamma$ which are valid when $\epsilon_q\gg|\Delta_{ij}|$. In our system $|\Delta_{ij}|=0.9$ meV. To obtain an estimate of ϵ_q we calculate $\epsilon_{\bar{q}}=\hbar^2\bar{q}^2/2m^*$ where $\bar{q}=5k_BT/\hbar\bar{v}_s$ is the dominant phonon wave number[19] and $\bar{v}_s=3368$ m/s is a suitable average value of the sound velocity.[33] For the temperature range of interest, $0.3-1.3$ K, we find that $\epsilon_{\bar{q}}$ varies between 2 and 37 meV and consequently is much larger than $|\Delta_{ij}|$.

The phonon-drag thermopower $S^g=-\Sigma_{ij}L_{ij}/\sigma$ is now written in the following form:

$$S^g=-\frac{L_{11}+L_{22}+L_{12}+L_{21}}{\sigma}=\frac{-e(2m^*)^{3/2}l_p\tau^{el}}{\sigma k_BT^2\hbar^4}\frac{V}{(2\pi)^3}\times\sum_s v_p^s\int_0^\infty\int_{-\infty}^\infty dq\,dq_zN^0_{\mathbf{Q}s}\epsilon_q\left\{[|U_{11}(\mathbf{Q}s)|^2+|U_{12}(\mathbf{Q}s)|^2]\int_\gamma^\infty d\epsilon_{\mathbf{k}}\frac{f_1^0(\epsilon_{\mathbf{k}})[1-f_1^0(\epsilon_{\mathbf{k}}+\hbar\omega_{\mathbf{Q}s})]}{\sqrt{\epsilon_{\mathbf{k}}-\gamma}}+[|U_{22}(\mathbf{Q}s)|^2+|U_{12}(\mathbf{Q}s)|^2]\times\int_\gamma^\infty d\epsilon_{\mathbf{k}}\frac{f_2^0(\epsilon_{\mathbf{k}})[1-f_2^0(\epsilon_{\mathbf{k}}+\hbar\omega_{\mathbf{Q}s})]}{\sqrt{\epsilon_{\mathbf{k}}-\gamma}}\right\}. \quad \text{(A21)}$$

At this stage, by omitting the complication of the screening effects, we can see that the square of the unscreened e-p interaction matrix elements are proportional to the form factors $|Z_{ij}(q_z)|^2$. In Fig. 7 we present the calculated values of $|Z_{11}(q_z)|^2$ (solid line), $|Z_{22}(q_z)|^2$ (dash-dotted line), and $|Z_{12}(q_z)|^2$ (dashed line). In the same figure we have plotted the form factor $|Z(q_z)|^2$ (dotted line) for a single well of width $W=18$ nm. We have calculated the average $\bar{q}_z$ of the phonons, which contribute to the intrasubband transitions, and we find that for the temperatures of our interest, $0.02<\bar{q}_z<0.04$ nm^{-1}. Moreover, $0.04<\bar{q}_z<0.1$ nm^{-1} and $0.08<\bar{q}_z<0.1$ nm^{-1} for the $1\rightarrow2$ and the $2\rightarrow1$ transitions respectively. From Fig. 7 we can see that for those small values of q_z the sum of $|Z_{ii}(q_z)|^2+|Z_{ij}(q_z)|^2$ (dash-dot-dotted line) is very close to $|Z(q_z)|^2$. Based on this simple result, S^g given by Eq. (A21) is practically the same as S^g for two 2DEG's with densities n_1 and n_2 and equal elastic relaxation times $\tau_1^{el}=\tau_2^{el}=\tau^{el}$ connected in parallel. The comparison between Eqs. (3) and (A21) is now straightforward.

[1] A. Palevski, F. Beltram, F. Capasso, L. Pfeiffer, and K. W. West, Phys. Rev. Lett. **65**, 1929 (1990).
[2] Y. Berk, A. Kamenev, A. Palevski, L. N. Pfeiffer, and K. W. West, Phys. Rev. B **50**, 15 420 (1994); M. Slutzky, O. Entin-Wohlman, Y. Berk, A. Palevski, and H. Shtrikman, *ibid.* **53**, 4065 (1996).
[3] R. J. Hyndman, S. T. Stoddart, B. Tieke, S. G. S. Lok, B. L. Gallagher, A. K. Geim, J. C. Maan and M. Henini, Physica B **251**, 745 (1998).
[4] S. K. Lyo, Phys. Rev. B **50**, 4965 (1994).
[5] A. Miele, R. Fletcher, E. Zaremba, Y. Feng, C. T. Foxon, and J. J. Harris, Phys. Rev. B **58**, 13 181 (1998).
[6] M. Tsaousidou, P. N. Butcher, and G. P. Triberis, Phys. Rev. B **64**, 165304 (2001).
[7] S. K. Lyo, Phys. Rev. B **38**, 6345 (1988).
[8] B. Tieke, R. Fletcher, U. Zeitler, M. Henini, and J. C. Maan, Phys. Rev. B **58**, 2017 (1998).
[9] R. Fletcher, M. Tsaousidou, P. T. Coleridge, Y. Feng, and Z. R. Wasilewski, Physica E (Amsterdam) **12**, 478 (2002).
[10] A. Gold and L. Calmels, Phys. Rev. B **48**, 11 622 (1993).
[11] L. Calmels and A. Gold, Phys. Rev. B **53**, 10 846 (1996).
[12] A. Gold, J. Phys.: Condens. Matter **13**, 11 641 (2001).
[13] B. Tanatar and B. Davoudi, Phys. Rev. B **63**, 165328 (2001).
[14] C. Bulutay and M. Tomak, Phys. Rev. B **53**, 7317 (1996).
[15] S. Moroni, D. M. Ceperley, and G. Senatore, Phys. Rev. Lett. **75**, 689 (1995).
[16] M. Tsaousidou, T. Smith, R. Fletcher, P. T. Coleridge, Z. R. Wasilewski, and Y. Feng, *Proceedings of the 26th International Conference on the Physics of Semiconductors (ICPS26), Edinburgh, 2002* (in press).
[17] S. Charlebois, J. C. Beerens, R. Côté, E. Lavallée, J. Beauvais, and Z. R. Wasilewski, Physica E (Amsterdam) **6**, 645 (2000).
[18] M. Tsaousidou, R. Fletcher, T. Smith, P. T. Coleridge, Z. R. Wasilewski, and Y. Fend (unpublished).
[19] B. L. Gallagher and P. N. Butcher, *Handbook on Semiconductors* (Elsevier, Amsterdam, 1992), Vol. 1. p. 721.
[20] D. G. Cantrell and P. N. Butcher, J. Phys. C **20**, 1985 (1987).
[21] P. N. Butcher and M. Tsaousidou, Phys. Rev. Lett. **80**, 1718 (1998).
[22] S. K. Lyo, Phys. Rev. B **40**, 6458 (1989).
[23] R. Fletcher, V. M. Pudalov, Y. Feng, M. Tsaousidou, and P. N. Butcher, Phys. Rev. B **56**, 12 422 (1997).
[24] T. Ando, A. B. Fowler, and F. Stern, Rev. Mod. Phys. **54**, 437 (1982).
[25] M. J. Smith and P. N. Butcher, J. Phys.: Condens. Matter **1**, 1261 (1989).
[26] B. Y.-K. Hu and S. Das Sarma, Phys. Rev. B **48**, 5469 (1993).
[27] K. Flensberg and B. Y.-K Hu, Phys. Rev. B **52**, 14 796 (1995).

[28] A.-P Jauho and H. Smith, Phys. Rev. B **47**, 4420 (1993).
[29] M. Jonson, J. Phys. C **9**, 3055 (1976).
[30] R. Pillarisetty, H. Noh, D. C. Tsui, E. P. De Poortere, E. Tutuc, and M. Shayegan, Phys. Rev. Lett. **89**, 016805 (2002).
[31] L. Swierkowski, J. Szymanski, and Z. W. Gortel, Phys. Rev. B **55**, 2280 (1997).
[32] S. Mori and T. Ando, Phys. Rev. B **19**, 6433 (1979).
[33] R. Fletcher, J. J. Harris, C. T. Foxon, M. Tsaousidou, and P. N. Butcher, Phys. Rev. B **50**, 14 991 (1994).